

(PCR) and cloned as described previously [25,26]. Positive clones with near full-length HIV-1 inserts were selected and the nucleotide sequences of HIV-1 genomes were determined on both strands by direct sequencing method with fluorescent dye terminators in an automated ABI PRISM310 DNA sequencer (Applied Biosystems, Inc., Foster City, California, USA), using the primer-walking approach.

Data analyses

The near full-length nucleotide sequences were aligned with the HIV-1 reference strains (<http://hiv-web.lanl.gov/HTML/alignments.html>), using CLUSTAL W version 1.4 [27], and corrected manually to ensure that gaps did not alter the reading frame. Phylogenetic trees were constructed by the neighbor-joining method [28] based on Kimura's two-parameter distance matrix with 100 bootstrap replicates [29] using PHYLIP, version 3.573 [30]. Bootscanning analysis [31] were performed on neighbor-joining trees for a window of 500 nucleotides moving along the alignment in increments of 100 nucleotides, using two different sets of reference sequences: A_92UG037, B'_RL42, C_95IN21068, D_NDK and CRF01_93TH253; A_Q23, B_HXB2, C_92BR025, D_94UG1141, and CRF01_90CF402. The analyses were implemented by the SIMPLOT 2.5 program [32]. To further define the precise boundaries of intersubtype recombination, informative site analysis was performed as described previously [33,34]. Confirmatory tree analyses were then carried out to explore the subtype origins of respective HIV-1 segments. Briefly, using the co-ordinates for the recombination breakpoints estimated by informative site analysis and bootscanning plots, HIV-1 genomes of the putative recombinants were divided into segments. Each segment was subjected to separate phylogenetic analyses using the neighbor-joining method to confirm the subtype or CRF origin of each segment. The 'predicted' parental sequences (B'_RL42, C_95IN21068

and CRF01_93TH253) for bootscanning and informative site analyses were selected based on the data obtained from confirmatory tree analysis.

Nucleotide sequence accession numbers

The near full-length nucleotide sequences reported in this article are available under the database accession numbers AB097865 to AB097873.

Results

High prevalence of HIV-1 strains with subtype discordance in Central Myanmar

HIV-1 genotypes of 59 specimens from Central Myanmar were determined by phylogenetic tree analyses based on the nucleotide sequences of *gag* (p17) and *env* (C2/V3) regions, using plasma HIV-1 RNAs. The distribution of HIV-1 genotypes in this population was as follows: 27 CRF01_AE (45.8%); 15 subtype B' (Thailand variant of subtype B) (25.4%); eight subtype C (13.6%). The remaining nine specimens (15.3%) showed the discordance between *gag* (p17) and *env* (C2/V3) subtypes (Table 1). The samples with subtype discordance were found most frequently among IDUs (six of 21, 28.6%) and fCSWs (two of 16, 12.5%), whereas none was detected among STD patients (none of 12) (Table 1).

To investigate the detailed structural features of HIV-1 strains in Mandalay, a total of 27 HIV-1 strains were isolated from these 59 HIV-1 samples. The relatively low isolation rate of HIV-1 (27 of 59, 45.8%) was due to the long-distance transportation of specimens. The genotype screening of these 27 isolates based on *gag* (p17) and *env* (C2/V3) regions identified 11 CRF01_AE (40.7%), seven subtype B' (26.0%) and four subtype C (14.8%), whereas the remaining five

Table 1. Summary of primary screening of HIV-1 genotypes^a in Central Myanmar.

Risk factor	Number subtyped	RF ^b								
		B'	C	CRF01_AE	RF ^b	B'/C	B'/01	C/B'	C/01	01/B'
IDU	21	7 (33.3%)	4 (19.0%)	4 (19.0%)	6 (28.6%)	1	1	1	2	1
Person with sexual exposure	38	8 (21.1%)	4 (10.5%)	23 (60.5%)	3 (7.9%)	0	1	1	0	1
CSW	16	2	0	12	2	0	0	1	0	1
STD	12	3	2	7	0	0	0	0	0	0
Hetero	10	3	2	4	1	0	1	0	0	0
Total	59	15 (25.4%)	8 (13.6%)	27 (45.8%)	9 (15.2%)	1	2	2	2	2

^aHIV-1 genotypes: HIV-1 subtype B', B'; subtype C, C; CRF01_AE, 01. ^bRF indicates the HIV-1 samples that show the discordance between *gag* (p17) and *env* (C2/V3) subtypes. The columns under RF show the breakdowns of the specimens with different profiles of subtype discordance. For example, B'/C indicates the HIV-1 sample that belongs to subtype B' in *gag* (p17) region and subtype C in *env* (C2/V3) region. IDU, injecting drug user; CSW, commercial sex worker; STD, sexually transmitted diseases; Hetero, heterosexual.

strains (18.5%) showed the diverse patterns of discordance between *gag* (p17) and *env* (C2/V3) subtypes, including *gag* subtype B' and *env* subtype C (99MM-mIDU106), B' and CRF01_AE (00MM-mIDU502), C and B' (00MM-mCSW503), C and CRF01_AE (99MM-mIDU107), and CRF01_AE and B' (99MM-mCSW104). Moreover, the additional genotyping based on nucleotide sequences of 3'-long terminal repeats (LTRs) found that one strain (99MM-mIDU103) assigned as subtype B' in the primary screening harbored the LTR of subtype C origin (see below). Taken together, our genotype screenings identified a total of six strains with subtype discordance (22.2%) among 27 isolates from Central Myanmar.

Highly diverse forms of unique intersubtype recombinants in Central Myanmar

To analyze the genome structures of these six HIV-1 isolates, we cloned and determined the near full-length nucleotide sequences of their proviral genomes. Three representative HIV-1 isolates from Central Myanmar that are presumably non-recombinant forms of subtypes B' (99MM-mSTD101) and C (99MM-mIDU101) and CRF01_AE (99MM-mCSW105) were analyzed in parallel for comparison. The 9.1 kb near full-length clones of six HIV-1 strains with subtype discordance were designated 99MM-mIDU106.18, 99MM-mCSW104.16, 99MM-mIDU107.34, 00MM-mIDU502.6, 00MM-mCSW503.2, and 99MM-mIDU103.10, and those of putative non-recombinant forms of HIV-1 subtypes B' and C and CRF01_AE strains are termed 99MM-mSTD101.8, 99MM-mIDU101.3 and 99MM-mCSW105.18, respectively. Whereas 99MM-mIDU101.3 carried a frame-shift mutation in the *gag* gene, other eight molecular clones had intact open reading frames for all nine HIV-1 genes.

The near full-length nucleotide sequences of these Mandalay isolates were subjected to recombination identification programs. The bootscanning analyses, using the reference strains of HIV-1 subtypes A (92UG037), B' (RL42), C (95IN21068), and D (NDK) and CRF01_AE (93TH253), revealed that all six HIV-1 strains with subtype discordance were highly diverse forms of unique recombinants comprised of various combinations of the segments derived from HIV-1 subtypes B' and C and CRF01_AE (Fig. 1a-f), whereas 99MM-mSTD101.8, 99MM-mIDU101.3 and 99MM-mCSW105.18 were indeed non-recombinant forms of HIV-1 subtypes B' and C and CRF01_AE, respectively (Fig. 1g-i). Similar results were obtained with an alternative set of reference sequences (A_Q23, B_HXB2, C_92BR025, D_94UG1141, 01_90CF402) (data not shown). To further define the recombination breakpoints, the informative site analysis was performed with predicted parental strains, including B'_RL42, C_95IN21068, and CRF01_93TH253. The informa-

tive site analysis gave high statistical support ($P < 0.001$) for all breakpoints (data not shown).

Next, we carried out the confirmatory tree analysis to examine the phylogenetic position of these newly identified recombinants in the respective HIV-1 segments and to estimate the origin of the viruses that have been involved in the recombinations (Fig. 2). The exact coordinates for the breakpoints relative to HXB2 were given in parentheses in Fig. 2. As shown in Fig. 2, the subtype structure deduced from confirmatory tree analysis was consistent with the results obtained from bootscanning (Fig. 1) and informative site analyses (data not shown). The deduced subtype structures are illustrated at the bottom of each panel in Figure 1. The confirmatory tree analysis also revealed that most of subtype B parts in these recombinants indeed belonged to subtype B' cluster and that the subtype C parts were closely-related phylogenetically to subtype C sequences from India (Fig. 2). However, the sequences in some fragments in 99MM-mIDU107.34 (Fig. 2e) and 00MM-mCSW503.2 (Fig. 2f) did not clearly cluster with the reference sequences for Indian subtype C (C_{IN}) and for CRF01_AE of Thai origin (01_{TH}). This is probably due to the poor resolution in the tree analysis because the fragments were too short (Fig. 2e and f). Alternatively, a few breakpoints may not be correctly identified. In fact, informative site analysis indicated that small patches of different subtypes appeared to be inserted in some segments (data not shown), although the analyses gave high statistical support for estimated subtype boundaries ($P < 0.001$). Of note, 00MM-mCSW503.2 was a particularly complex chimera that contained at least 13 recombination breakpoints between subtypes B' and C and CRF01_AE (Figs 1f and 2f). This would be one of the most complex chimeras ever reported.

Mandalay URFs with "pseudotype" virion structures

Intriguingly, some of recombinant strains identified in the present study showed 'pseudotype' virion structures, in which the external portions of the envelope glycoproteins were exchanged with that of different lineage of HIV-1 strains. The most distinct examples were a pair of 00MM-mIDU502.6 (Fig. 1b) and 99MM-mCSW104.16 (Fig. 1c), that showed reciprocal patterns of recombination between subtype B' and CRF01_AE. The 00MM-mIDU502.6 was a subtype B' strain recombined with CRF01_AE in the external portion of the envelope glycoprotein (Fig. 1b). In contrast, the 99MM-mCSW104.16 was a CRF01_AE strain recombined with the external portion of the envelope glycoprotein of subtype B' (Fig. 1c). Similarly, the 99MM-mIDU106.18, that was comprised mostly of subtype B', was recombined with the external portion of the envelope glycoprotein of subtype C origin (Fig. 1d). Although the subtype

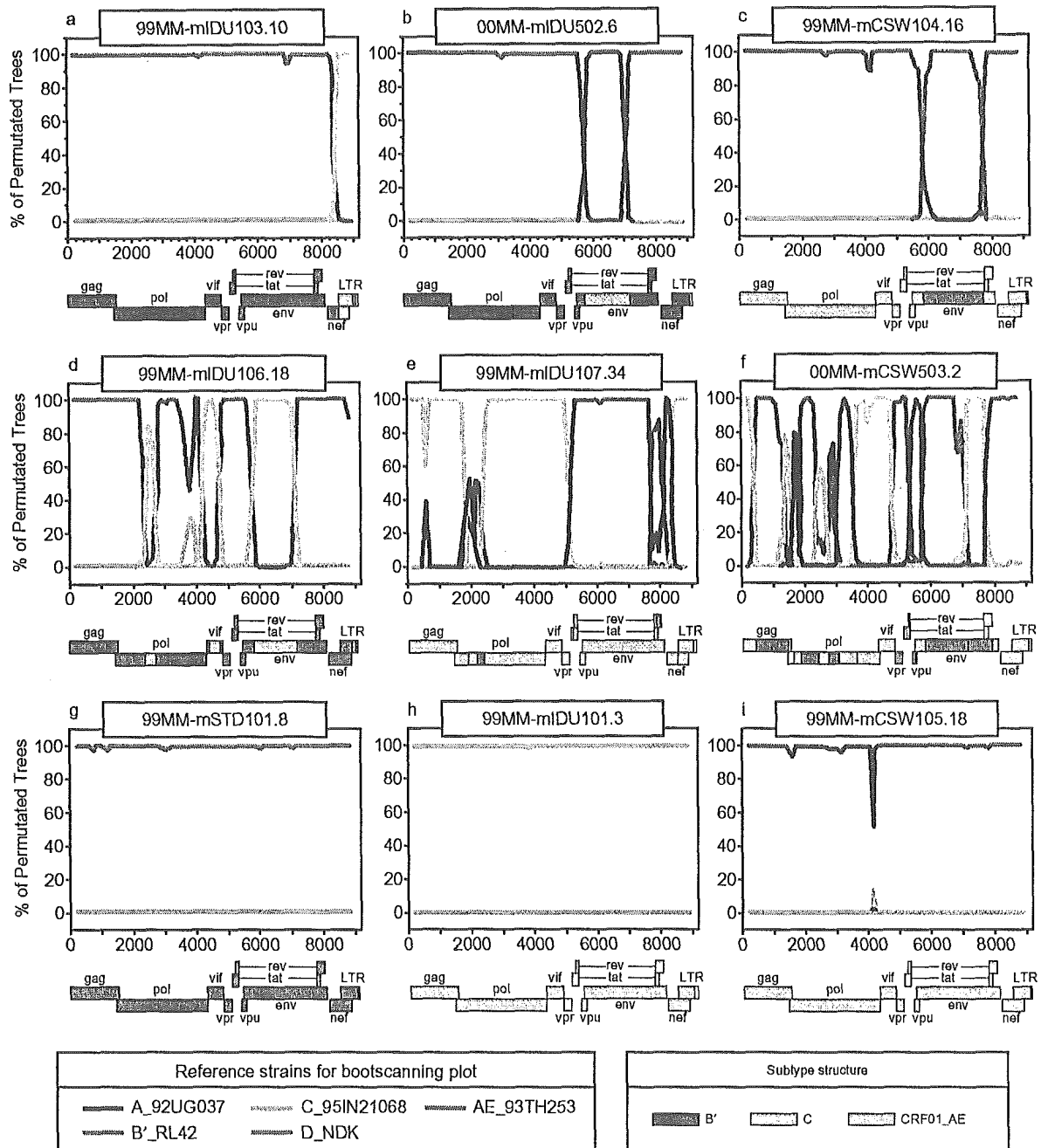


Fig. 1. Bootscanning plots and deduced subtype structures of near full-length genome sequence of HIV-1 isolates from Mandalay (Central Myanmar). The bootscanning plots, depicting the relationship of Mandalay isolates to the reference strains of HIV-1 subtypes A (92UG037), B' (RL42), C (95IN21068), and D (NDK) and CRF01_AE (93TH253) (indicated in the inset at the bottom left) are shown. The bootstrap values are plotted for a window of 500 bp moving in increments of 100 bp along the alignment. The deduced subtype structure is illustrated at the bottom of each panel. The regions of the respective subtypes are shown in different colors indicated at the bottom right. The long terminal repeat (LTR) region of 99MM-mIDU106.18 was found to contain small subtype C segment in the enhancer–promoter region (see text). The exact coordinates for the recombination breakpoints are given in the parenthesis in Fig. 2.

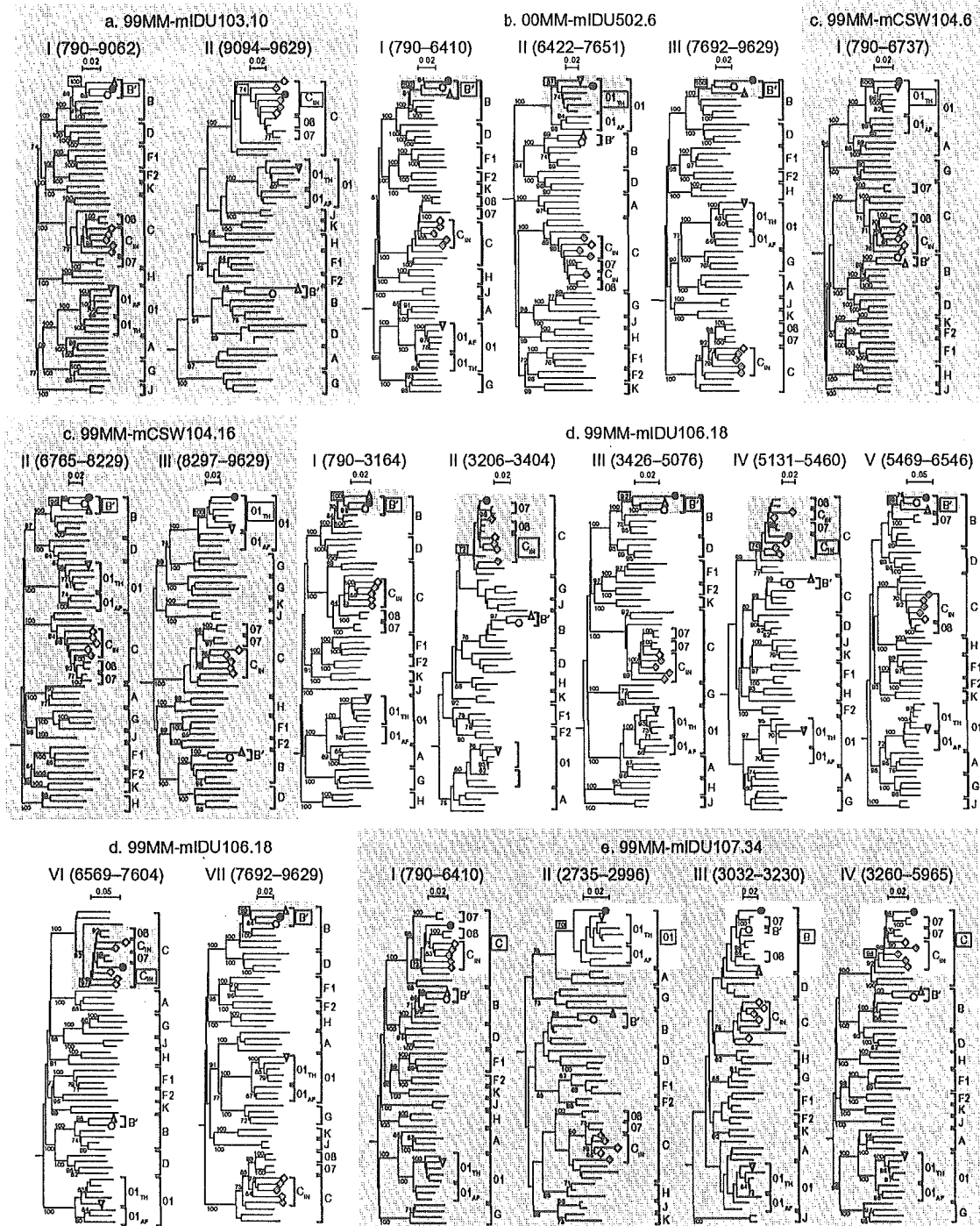
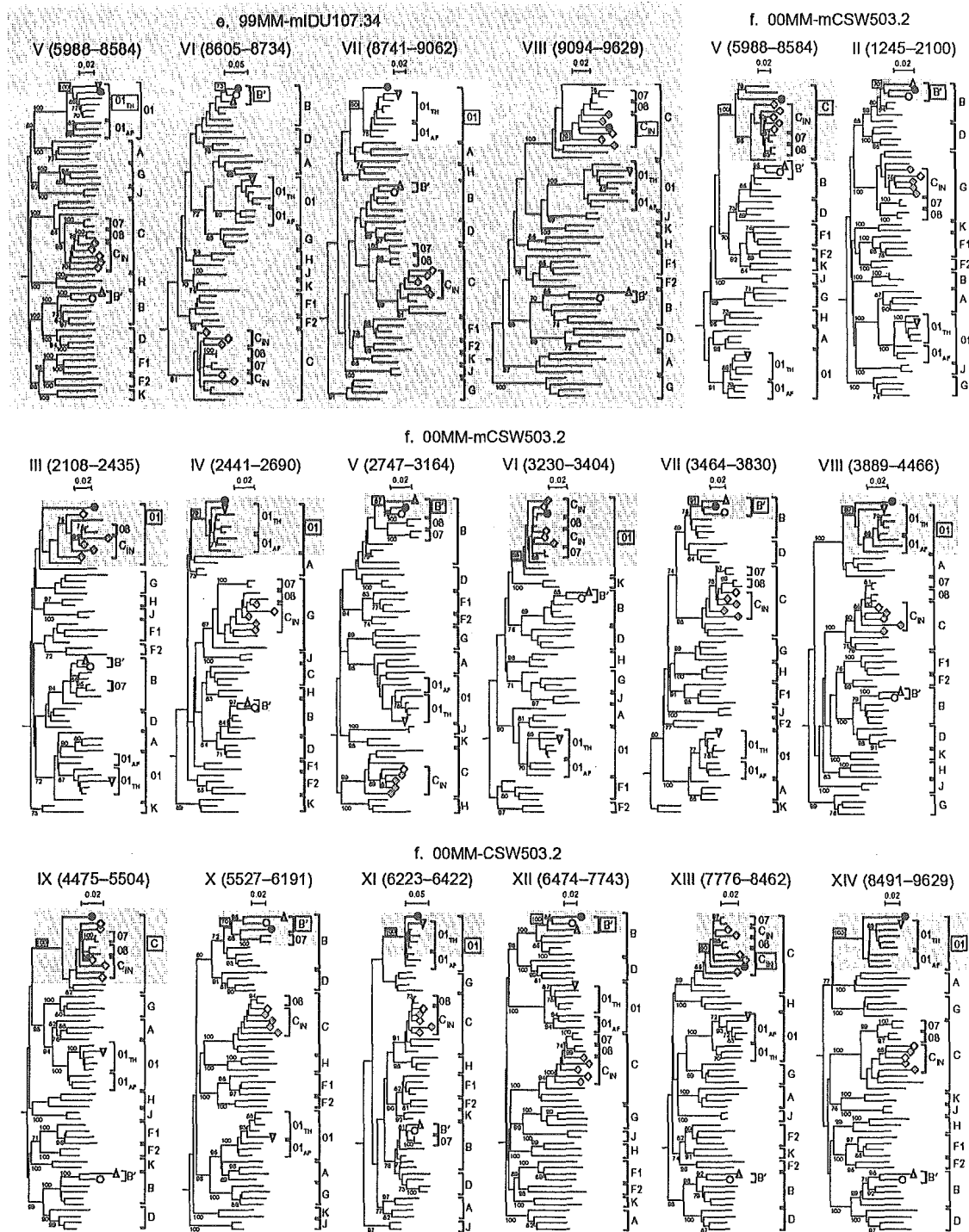


Fig. 2. Confirmatory tree analysis. Using the coordinates for the recombination breakpoints identified by the informative site analysis, HIV-1 genomes were divided into segments numbered by Roman numerals. Each segment was subjected to separate phylogenetic analyses based on neighbor-joining method to confirm the subtype or circulating recombinant form (CRF) origin of segment. The stability of the nodes was assessed by using maximum parsimony [30] with the bootstrap value of 100 replications [29]. Bootstrap values 70% or higher of key nodes are shown. *SIV_{CPZ}GAB* was used as an outgroup but is not shown for simplicity. The coordinates of each segment (shown in the parentheses at the top of each tree) are given relative to the HXB2 genome (<http://hiv-web.lanl.gov/content/hiv-db/NUM-HXB2/HXB2.MAIN.html>). The analysis starts from *gag* open reading



frame. The bootstrap values, with which the cluster containing each query strain (closed circle) is supported, are marked within the squares at the corresponding nodes. The genotype assignments of each query strain in the respective phylogenetic analyses are indicated in the box at the right-hand side of each panel. Non-recombinant forms of subtypes B' (99MM-mSTD101.8, open triangle) and C (99MM-mIDU101.3, open diamond) and CRF01_AE (99MM-mCSW105.18, open inverted triangle) identified in the present study were also included. B', subtype B' (Thailand variant of subtype B; B'_CN.RL42, open circle); C_{IN}, India cluster of subtype C (93IN905, 95IN21068, 98IN012 and 98IN022; striped diamond); 01, CRF01_AE; 01_{TH}, Thailand CRF01; 01_{AF}, African CRF01; 07, CRF07_BC; 08, CRF08_BC.

structure was less simple, 99MM-mIDU107.34, that was comprised mainly of subtype C, was recombined with CRF01_AE in *env* region (Fig. 1e). Even in the most complex chimera, 00MM-mCSW503.2, we saw a similar trend. In 00MM-mCSW503.2, the external portion of the envelope glycoprotein of subtype B' origin appeared to be recombined with a chimeric genome with highly complex subtype composition (Fig. 1f and 2f). One exception was 99MM-mIDU103.10, that was a chimera comprised mostly of subtype B' with a small segment (approximately 200 bp) derived from subtype C in LTR region (Fig. 1a and 2a, see below).

Phylogenetic relationship of HIV-1 strains from Central Myanmar

The neighbor-joining tree analysis based on near full-length nucleotide sequences revealed that HIV-1 intersubtype chimeras were the 'outliers' placed outside the clusters of known HIV-1 subtypes or CRFs, whereas three putative non-recombinant forms of HIV-1 strains formed monophyletic clusters with subtypes B' and C and CRF01_AE, respectively (Fig. 3). The locations of HIV-1 recombinants in the phylogenetic tree appeared

to reflect the proportion of the length of each subtype segment in respective HIV-1 chimera. For instance, 00MM-mIDU502.6 and 99MM-mIDU107.34 and 99MM-mCSW104.16 which were made up mainly of subtype B', C and CRF01_AE (Fig. 1) were located near the clusters of subtype C and CRF01_AE, respectively (Fig. 3). In contrast, the highly complex chimera, 00MM-mCSW503.2, that was made up of multiple segments of subtypes B' and C and CRF01_AE, branched out from the central part of the tree (Fig. 3). Of note, a subtype C strain from Central Myanmar (99MM-mIDU101.3) was most closely related to those of Indian origin (95IN21068 and 93IN905) (Fig. 3) [23].

Discussion

The present study revealed that substantial portions of HIV-1 strains circulating in the city of Mandalay in Central Myanmar were URFs with diverse profiles of intersubtype recombinations (Fig. 1, Table 1). They were not related each other nor to any known

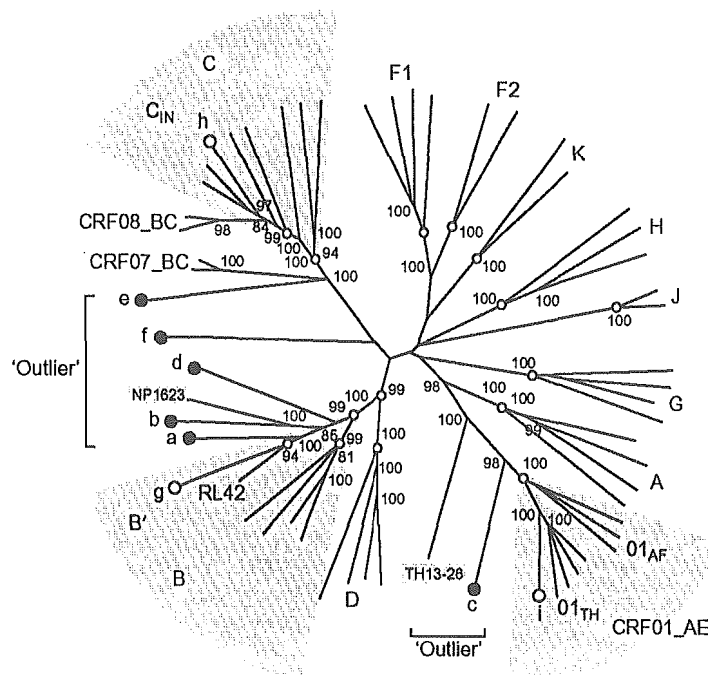


Fig. 3. Phylogenetic relationship of the diverse forms of unique HIV-1 intersubtype recombinants isolated in Central Myanmar. Neighbor-joining tree based on near full-length nucleotide sequences is shown with the reference strains for HIV-1 group M (subtypes A–D, F–H, J, and K) and circulating recombinant forms (CRFs) as well as the recently reported recombinants between subtype B' and CRF01_AE identified in Thailand (97TH.NP1623 [17] and TH13-26, shadowed). SIV_{CPZ}GAB was used as an outgroup but is not shown for simplicity. Subtype and CRF designations are indicated outside the tree. Bootstrap values greater than 90 are shown at corresponding nodes. HIV-1 unique recombinant forms (closed circle): a, 99MM-mIDU103.10; b, 00MM-mIDU502.6; c, 99MM-mCSW104.16; d, 99MM-mIDU106.18; e, 99MM-mIDU107.34; f, 00MM-mCSW503.2. Non-recombinant forms of subtype B' (g, 99MM-mSTD101.8), subtype C (h, 99MM-mIDU101.3) and CRF01_AE (i, 99MM-mCSW105.18) strains from Central Myanmar (open circle). HIV-1 genotype notations are same as in Figure 2.

recombinants, indicating that they had arisen independently. The prevalence of URFs among high risk population in Central Myanmar is approximately 10 % in CSWs and 20–30 % in IDUs (Table 1) [20,23,35]. Since our screening system for HIV-1 genotypes relied on the nucleotide sequencing of *gag* (p17) and *env* (C2/V3) regions, the actual numbers of HIV-1 intersubtype recombinants in Central Myanmar could be greater than we reported in the present study. Indeed, by additional genotype screening based on 3'-LTR, we identified one B'/C recombinant (99MM-mIDU103.10) (Fig. 1a) among four HIV-1 isolates that were originally assigned as subtype B'. Obviously, the more HIV-1 segments are analyzed, the more recombinants are likely to be recognized in this study site. As seen in 00MM-mCSW503.2 (with 13 recombination breakpoints) (Fig. 1f) and 99MM-mIDU107.34 (with seven recombination breakpoints) (Fig. 1e), some Mandalay URFs were highly complex chimeras between multiple lineages of HIV-1 strains. These findings, taken together, suggest that extensive recombination events are taking place in an ongoing fashion and new recombinants appeared to be arising continually in this area. Similar phenomenon was observed in Central Africa, where the proportion of discordant *gag/env* samples account for up to 40% [36].

This unusually high rate of detection of intersubtype recombinants is not due to the technical artifacts, including the possibility of the template switch during the long PCR procedure. We scrutinized the recombination breakpoints by determining the nucleotide sequences of original virus stocks and plasma samples in separate experiments. The results were consistent with the data obtained from near full-length DNA clones in the present study.

The exploratory tree analysis gave further information on the origin of the viruses that have been involved in the recombinations. As shown in Figure 2, exploratory analyses demonstrated that most of subtypes B and C and CRF01_AE parts of recombinant genomes belonged to the clusters of subtype B' (Thailand variant of subtype B), subtype C of India origin, and Thailand CRF01_AE, respectively, indicating that newly emerged recombinants in Central Myanmar have been generated by the mixing of subtype B' and CRF01_AE from Thailand and the subtype C strains from India (Fig. 4).

A geographical hot spot of extensive HIV-1 intersubtype recombination events has been recently identified in the western part (Dehong Prefecture) of Yunnan Province in China, near the border to Myanmar, where approximately two-thirds of circulating strains are URFs mainly comprised of subtypes B' and C [18] (Fig. 4). The high prevalence of URFs in Central Myanmar and the western part of Yunnan Province of

China are likely to reflect the presence of highly exposed individuals and social networks of HIV-1 transmissions in these areas [18]. The areas, including western Yunnan and Central Myanmar, thus appear to be the 'melting pots' where the diverse forms of HIV-1 recombinants are continually generated (Fig. 4).

As typically seen in CRF01_AE (*env* E in subtype A backbone), and CRF14_BG (*env* B in subtype G backbone), some CRFs exhibited 'pseudotype' virion structures, in which the external portions of the envelope glycoprotein were exchanged with that of different lineage of HIV-1 strain. A similar tendency was observed in other CRFs with more complex recombinant structure, including CRF02_AG (*env* A in subtypes A/G backbone), CRF06_cpx (*env* G in subtypes A/J/K backbone), CRF011_cpx (*env* A in subtypes A/E/G/J backbone), and CRF13_cpx (*env* A in subtypes A/E/G/J/U backbone). Intriguingly, approximately half of Mandalay URFs (four of six) identified in the present study displayed such 'pseudotype' virion structures (Fig. 1).

Tovanabutra *et al.* has identified one recombinant (97TH.NP1623), in which the external portion of *env* gene of CRF01_AE were exchanged with subtype B' genome, in a multiply exposed individual in Thailand [17]. Although the subtype structure of 97TH.NP1623 resembles that of 00MM-mIDU502.6, the precise locations of recombination breakpoints are not identical, indicating that both recombinants have been generated independently. This may also suggest that there are the mechanism(s) to allow the convergent evolution of recombinants with virtually identical configuration, albeit they seem to be generated independently in two epidemiologically-unrelated individuals. It is thus tempting to speculate that such 'pseudotype' virion structures might confer potential selective advantage on recombinant viruses over parental viruses (e.g. to escape from host immune surveillance), leading to the evolution of the recombinants with nearly identical subtype structures.

In summary, the present study identified the unique geographical hot spot in Central Myanmar where the extensive recombinations appear to be taking place continually. The presence of highly exposed individuals and social networks of HIV-1 transmission could quickly lead to the generation of highly diverse forms of unique intersubtype recombinants. This provides insights into the understanding the genesis of HIV-1 epidemic in this particular area in Asia.

Acknowledgements

We would like to thank Pe Thet Htoon, Min Thwe, Soe Lwin, Khin Yi Oo, the staff at the Ministry of

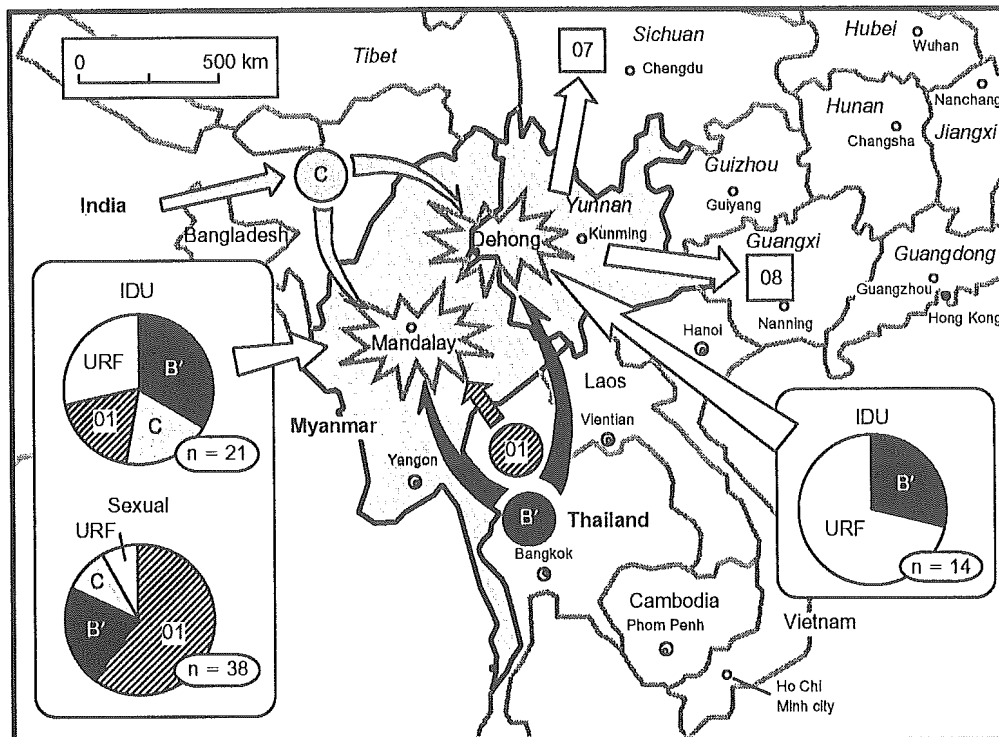


Fig. 4. Geographical hot spots of extensive recombinations between circulating HIV-1 subtypes in Southeast Asia. Western Yunnan (Dehong Prefecture) and Central Myanmar (Mandalay) (marked with 'explosion' symbols) are the 'melting pots' where extensive recombinations between different lineages of HIV-1 strains appear to be taking place continually. The pies show the prevalence of respective HIV-1 genotypes at the indicated study sites. The data for western Yunnan Province of China were adopted from the study reported by Yang *et al.* [18]. Plausible routes of HIV-1 spread are schematically illustrated. B', subtype B'; C, subtype C; IDU, injecting drug users; URF, unique recombinant form; 01, CRF01_AE; 07, CRF07_BC; 08, CRF08_BC.

Health of Myanmar, Naoki Yamamoto and Yoshiyuki Nagai for their support and Tim Mastro for his critical reading of the manuscript. We also thank Rongge Yang, Teichiro Shiino, Yuko Imamura and Kayoko Kato for their help and discussion, and Midori Kawasaki for preparation of the manuscript.

Sponsorship: This study was supported by the grants from the Ministry of Health, Labour and Welfare, the Ministry of Education, Science and Technology, and the Japanese Foundation for AIDS Prevention.

References

- Preston BD, Poiesz BJ, Loeb LA. Fidelity of HIV-1 reverse transcriptase. *Science* 1988, 242:1168-1171.
- Mansky LM. Retrovirus mutation rates and their role in genetic variation. *J Gen Virol* 1998, 79:1337-1345.
- Ho DD, Neumann AU, Perelson AS, Chen W, Leonard JM, Markowitz M. Rapid turnover of plasma virions and CD4 lymphocytes in HIV-1 infection. *Nature* 1995, 373:123-126.
- Wei X, Ghosh SK, Taylor ME, Johnson VA, Emami EA, Deutsch P, *et al.* Viral dynamics in human immunodeficiency virus type 1 infection. *Nature* 1995, 373:117-122.
- Perelson AS, Neumann AU, Markowitz M, Leonard JM, Ho DD. HIV-1 dynamics in vivo: virion clearance rate, infected cell life-span, and viral generation time. *Science* 1996, 271:1582-1586.
- Goodrich DW, Duesberg PH. Retroviral recombination during reverse transcription. *Proc Natl Acad Sci USA* 1990, 87: 2052-2056.
- Hu WS, Temin HM. Retroviral recombination and reverse transcription. *Science* 1990, 250:1227-1233.
- Stuhlmann H, Berg P. Homologous recombination of copackaged retrovirus RNAs during reverse transcription. *J Virol* 1992, 66: 2378-2388.
- Malim MH, Emerman M. HIV-1 sequence variation: drift, shift, and attenuation. *Cell* 2001, 104:469-472.
- Carr JK, Salminen MO, Albert J, Sanders-Buell E, Gotte D, Bix DL, *et al.* Full genome sequences of human immunodeficiency virus type 1 subtypes G and A/G intersubtype recombinants. *Virology* 1998, 247:22-31.
- Carr JK, Laukkanen T, Salminen MO, Albert J, Alaeus A, Kim B, *et al.* Characterization of subtype A HIV-1 from Africa by full genome sequencing. *AIDS* 1999, 13:1819-1826.
- Kuiken CL, Foley B, Hahn B, Marx P, McCutchan F, Mellor J, *et al.* (eds). *Human Retroviruses and AIDS*. Los Alamos, NM: Los Alamos National Laboratory; 1999.
- McCutchan FE. Understanding the genetic diversity of HIV-1. *AIDS* 2000, 14 (suppl 3):S31-44.
- Salminen MO, Carr JK, Robertson DL, Hegerich P, Gotte D, Koch C, *et al.* Evolution and probable transmission of intersubtype recombinant human immunodeficiency virus type 1 in a Zambian couple. *J Virol* 1997, 71:2647-2655.
- Neilson JR, John GC, Carr JK, Lewis P, Kreiss JK, Jackson S, *et al.* Subtypes of human immunodeficiency virus type 1 and disease stage among women in Nairobi, Kenya. *J Virol* 1999, 73: 4393-4403.

16. Lole KS, Bollinger RC, Paranjape RS, Gadkari D, Kulkarni SS, Novak NG, *et al.* Full-length human immunodeficiency virus type 1 genomes from subtype C-infected seroconverters in India, with evidence of intersubtype recombination. *J Virol* 1999, 73:152–160.
17. Tovnanabutra S, Polonis V, De Souza M, Trichavaroj R, Chanbancherd P, Kim B, *et al.* First CRF01_AE/B recombinant of HIV-1 is found in Thailand. *AIDS* 2001, 15:1063–1065.
18. Yang R, Xia X, Kusagawa S, Zhang C, Ben K, Takebe Y. Ongoing generation of multiple forms of HIV-1 intersubtype recombinants in the Yunnan Province of China. *AIDS* 2002, 16:1401–1407.
19. Htoon MT, Lwin HH, San KO, Zan E, Thwe M. HIV/AIDS in Myanmar. *AIDS* 1994, 8:S105–109.
20. Kusagawa S, Sato H, Watanabe S, Nohtomi K, Kato K, Shino T, *et al.* Genetic and serologic characterization of HIV type 1 prevailing in Myanmar (Burma). *AIDS Res Hum Retroviruses* 1998, 14:1379–1385.
21. UNAIDS. *United Nations response to HIV/AIDS in Myanmar: the United Nations joint plan of action 2001–2002*. Geneva, Switzerland: UNAIDS; 2001.
22. UNAIDS/WHO. *AIDS Epidemic Update December 2001*. Geneva: UNAIDS/WHO; 2001.
23. Motomura K, Kusagawa S, Kato K, Nohtomi K, Lwin HH, Tun KM, *et al.* Emergence of new forms of human immunodeficiency virus type 1 intersubtype recombinants in central Myanmar. *AIDS Res Hum Retroviruses* 2000, 16:1831–1843.
24. Kato K, Sato H, Takebe Y. Role of naturally occurring basic amino acid substitutions in the human immunodeficiency virus type 1 subtype E envelope V3 loop on viral coreceptor usage and cell tropism. *J Virol* 1999, 73:5520–5526.
25. Salminen MO, Koch C, Sanders-Buell E, Ehrenberg PK, Michael NL, Carr JK, *et al.* Recovery of virtually full-length HIV-1 provirus of diverse subtypes from primary virus cultures using the polymerase chain reaction. *Virology* 1995, 213:80–86.
26. Kusagawa S, Takebe Y, Yang R, Motomura K, Ampofo W, Brandful J, *et al.* Isolation and characterization of a full-length molecular DNA clone of Ghanaian HIV type 1 intersubtype A/G recombinant CRF02_AG, which is replication competent in a restricted host range. *AIDS Res Hum Retroviruses* 2001, 17:649–655.
27. Thompson JD, Higgins DG, Gibson TJ. CLUSTAL W: improving the sensitivity of progressive multiple sequence alignment through sequence weighting, position-specific gap penalties and weight matrix choice. *Nucl Acids Res* 1994, 22:4673–4680.
28. Saitou N, Nei M. The neighbor-joining method: a new method for reconstructing phylogenetic trees. *Mol Biol Evol* 1987, 4:406–425.
29. Felsenstein J. Confidence limits on phylogenies: an approach using the bootstrap. *Evolution* 1985, 39:783–791.
30. Felsenstein J. *PHYLIP (Phylogeny Inference Package) version 3.5c*. Seattle: Department of Genetics, University of Washington; 1993.
31. Salminen MO, Carr JK, Burke DS, McCutchan FE. Identification of breakpoints in intergenotypic recombinants of HIV type 1 by bootscanning. *AIDS Res Hum Retroviruses* 1995, 11:1423–1425.
32. Ray SC. *SIMPLOT FOR WINDOWS, version 2.5*. (distributed by author via <http://www.welch.jhu.edu/~sray/download>) Johns Hopkins Medical Institutions, Baltimore, MD, USA. 1999.
33. Gao F, Robertson DL, Caruthers CD, Morrison SG, Jian B, Chen Y, *et al.* A comprehensive panel of near-full-length clones and reference sequences for non-subtype B isolates of human immunodeficiency virus type 1. *J Virol* 1998, 72:5680–5698.
34. Robertson DL, Sharp PM, McCutchan FE, Hahn BH. Recombination in HIV-1. *Nature* 1995, 374:124–126.
35. Motomura K, Kusagawa S, Lwin HH, Thwe M, Kato K, Oishi K, *et al.* Different subtype distributions in two cities in Myanmar: Evidence for independent clusters of HIV-1 transmission. *AIDS* 2002, 16:633–636.
36. Peeters M. Recombinant HIV sequences: their role in the global epidemic. In *Human Retroviruses and AIDS: a compilation and Analysis of Nucleic Acid and Amino Acid sequences*. Edited by Kuiken C, Foley B, Hahn B, Marx P, McCutchan F, Mellors J, *et al.* Los Alamos, NM: Los Alamos National Laboratory; 2000: 54–72.

Sequence Note

Identification of HIV Type 2 Subtype B Transmission in East Asia

SHIGERU KUSAGAWA,¹ YUKO IMAMURA,¹ AKIRA YASUOKA,²
HIROO HOSHINO,³ SHIN-ICHI OKA,² and YUTAKA TAKEBE¹

ABSTRACT

We isolated an HIV-2 strain (01JP-IMCJ/KR020) from a Korean patient who has lived in Japan for the past 6 years. He was infected with HIV-2 through heterosexual contacts in either Korea or Japan. The phylogenetic analyses based on the near full-length nucleotide sequence revealed that 01JP-IMCJ/KR020 belongs to HIV-2 subtype B cluster with high bootstrap support. This isolate harbors a 13-nucleotide insertion upstream of the NF- κ B site, which is one of the sequence signatures specific to HIV-2 subtype B. This represents the first report of HIV-2 subtype B transmission in East Asia; three cases of HIV-2 subtype A infection have been reported in Korea in 1991–1998. This suggests that at least sporadic transmission of HIV-2, including both subtypes A and B, occurs in East Asia. It is necessary to keep monitoring HIV-2 to see whether there is an increasing trend toward HIV-2 infection in this particular area in Asia.

INTRODUCTION

HUMAN IMMUNODEFICIENCY VIRUS TYPE 2 (HIV-2) infections are endemic in West Africa, and are also found in India, Brazil, and Europe.¹ HIV-2-infected individuals may exhibit longer clinical latency periods and slower disease progression.^{2–4} The sexual and perinatal transmissions of HIV-2 are much less efficient than HIV-1 and this may be attributed to a low viral burden during the relatively long asymptomatic period.^{5–7} This may be the reason why the number of HIV-2-infected individuals has remained small, confined to limited geographic regions compared to HIV-1 infection.

HIV-2s are known to be members of a broader HIV-2 simian immunodeficiency virus (SIV_{SM}) phylogenetic group. SIV_{SM} in sooty mangabeys are linked to cross-species transmissions and an origin for HIV-2 infection in humans.^{8,9} HIV-2/SIV_{SM} phylogenetic groups were classified into seven genetic subtypes, A through G.^{8,9} Only HIV-2 subtypes A and B are disseminated into significant numbers of human populations. HIV-2 subtype A has been identified predominantly in the western

part of West Africa, including Guinea Bissau, Senegal, Gambia, and Mali. In contrast, HIV-2 subtype B has been found in central and eastern West African countries, including Ivory Coast, Ghana, and Nigeria.^{1,10}

In Asia, HIV-2 infections are present in West India, frequently associated with dual infections of HIV-1 subtype C strains.^{11,12} Outside India, five cases of HIV-2 infections have been documented in Korea. Among them, three cases were confirmed to be HIV-2 subtype A infections.¹³ The present study describes the identification of the first case of HIV-2 subtype B transmission in East Asia and discusses its structural properties based on near full-length nucleotide sequence and on the epidemiology of HIV in this region.

A 42-year-old man Korean national presented to a hospital in Tokyo in June 2001 with a dry cough, mild fever (37.1°C), and weight loss (a reduction of 3 kg from 66 kg in the last year). He lived in Japan as a construction worker for 6 years (1994 to 1997 and May 1999 to January 2002), returning to Korea in 1997–1999. He was unmarried and had a past history of gonorrhea around 1980. The patient manifested pulmonary tuber-

¹Laboratory of Molecular Virology and Epidemiology, AIDS Research Center, National Institute of Infectious Diseases, Tokyo 162-8640, Japan.

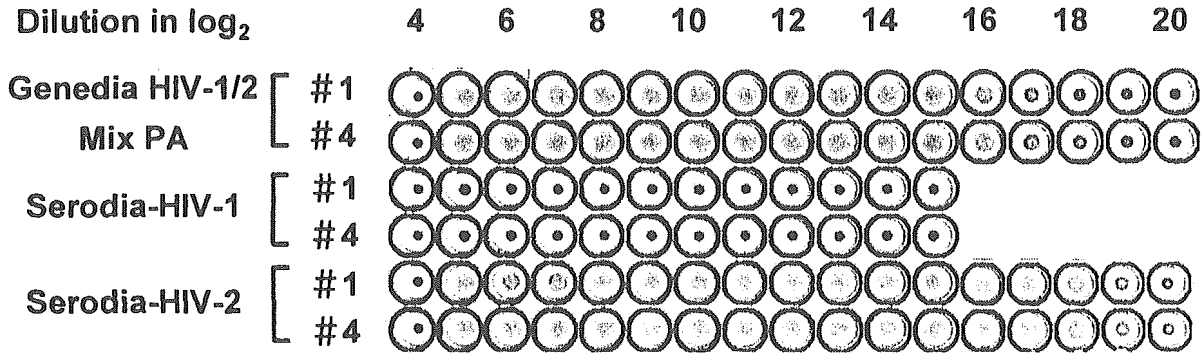
²AIDS Clinical Center, International Medical Center of Japan, Tokyo 162-8655, Japan.

³Department of Hygiene, Faculty of Medicine, Gunma University, Gunma 371-8511 Japan.

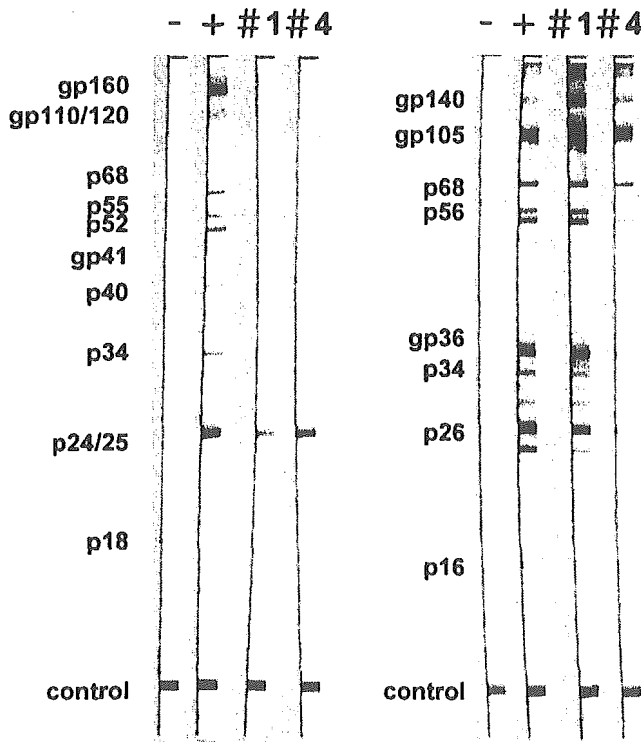
culosis and low CD4⁺ T lymphocyte counts (276 cells/ μ l) on admission. An HIV screening test using the Genedia HIV-1/2 Mix gelatin particle agglutination (PA) test (Fujirebio, Tokyo, Japan) showed strong HIV positivity with a titer of 1:10⁵ (Fig. 1A, top). The HIV-type-specific PA tests to distinguish HIV-1 and HIV-2 infections using gelatin particles individually coated with either HIV-1 or HIV-2 antigens (Serodia-HIV-1 and -HIV-

2, Fujirebio, Tokyo, Japan) exhibited a high titer (1:10⁵) of agglutination reaction only to HIV-2-coated particles (Fig. 1A, middle), showing no agglutination reaction to HIV-1-coated particles (Fig. 1A, bottom). Western blot analyses, using Lab-blot 1 and Lab-blot 2 (Fig. 1B), and PEPTILAV 1-2 peptide-based serological tests (Bio-Rad-Fujirebio, Tokyo, Japan) (Fig. 1C) unequivocally confirmed HIV-2 infection without any sero-

(A)



(B) LAV-Blot 1 LAV-Blot 2



(C)

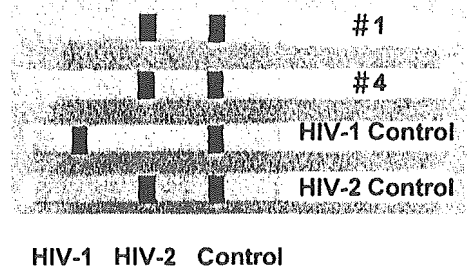


FIG. 1. Serological confirmation of HIV-2 infections. (A) Particle agglutination (PA) tests, using Genedia HIV-1/2 Mix PA test kits for screening of HIV infections (top), and discriminative PA tests, using gelatin particles coated with HIV-1 (middle) and HIV-2 (bottom) antigens. (B) Confirmatory Western blot analyses for detection of HIV-1 (left: LAV-Blot 1) and HIV-2 (right: LAV-Blot 2) infections. +, HIV-1 or HIV-2-positive control serum; -, negative control serum. (C) Peptide-based assays (PEPTILAB 1 and 2) to discriminate HIV-1 and HIV-2 infection. #1 and #4 were the plasma specimens taken from the patient at two different time points.

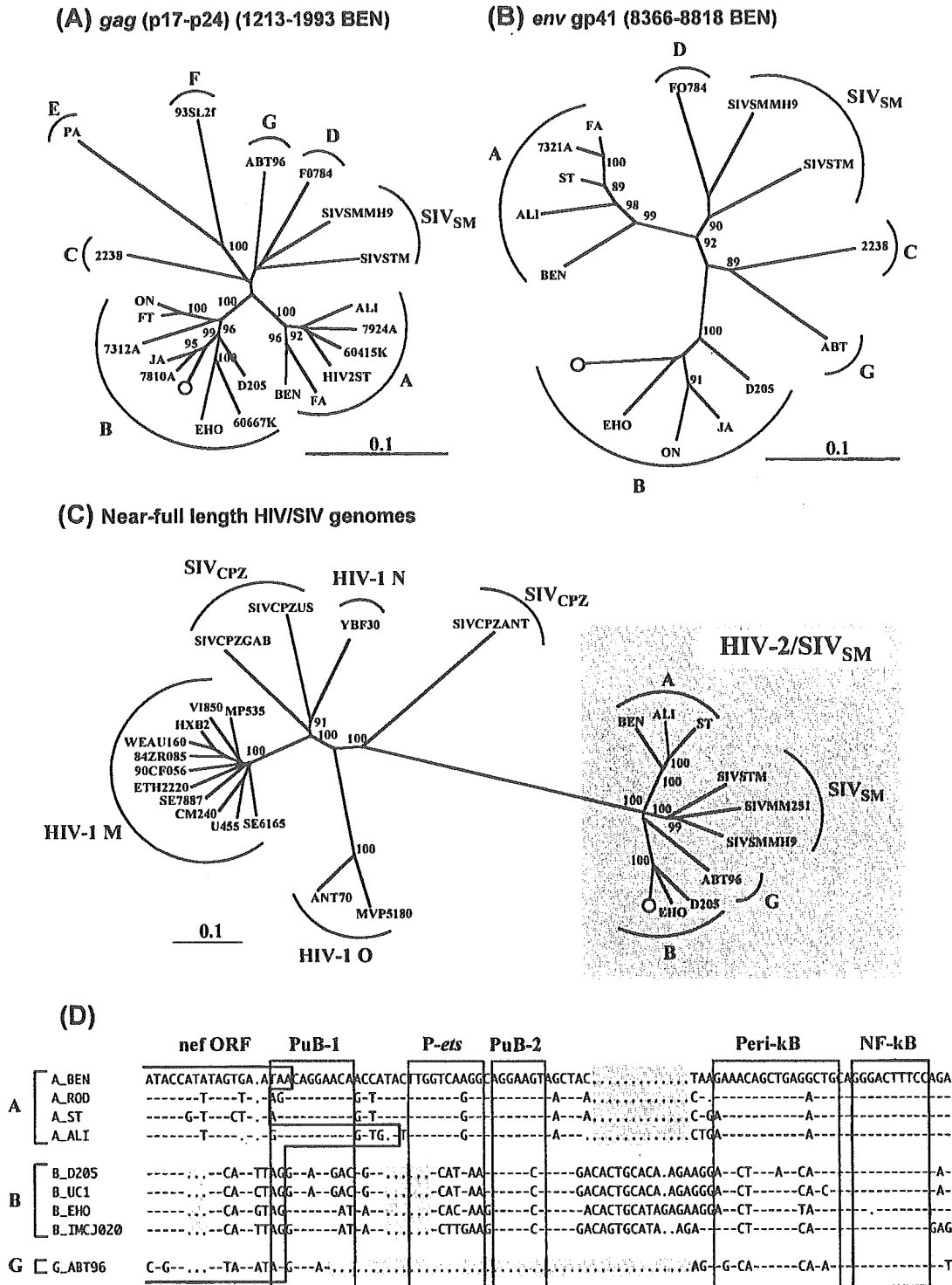


FIG. 2. Phylogenetic relationship and subtype-specific sequence signatures of HIV-2 subtype B strain (01JP-IMCJ/KR020) identified in East Asia. Phylogenetic trees were constructed by a neighbor-joining method using maximum likelihood distances calculated under the Felsenstein 84 model, based on the nucleotide sequences of *gag* (p17–p24) (A), *env* (p41) (B), and 9.1-kb near full-length proviral genome (C) with HIV/SIV reference sequences (<http://hiv-web.lanl.gov>). The analyses were implemented by PHYLIP version 3.6a3. The bootstrap values (100 replications) are shown at the corresponding nodes. (D) Subtype-specific differences in the nucleotide sequences of the enhancer regions of LTR in various HIV-2 strains. Dashes (–) indicates the sequence identity with HIV-2 subtype A reference strain (BEN). Dots (●) denote the gaps introduced to improve the alignment. Gaps that appear to be specific to HIV-2 subtype B strains are shaded. The sequence landmarks, including HIV-2 U3 LTR transcription factor elements and *nef* open reading frames, are shown.

logical cross-reactivity to HIV-1. While amplifications of HIV genomes through polymerase chain reaction (PCR) and RNA-PCR were repeatedly unsuccessful for both peripheral blood mononuclear cells (PBMCs) and plasma specimens by previously described primers,⁹ HIV-2 sequences were eventually amplified by PCR using newly designed primer sets for HIV-2 envelope transmembrane portions: 2TM051A (sense, 5'-CCCGGACTTTACTGGCTGGGATAGTGC-3' (nucleotide position 8319–8345, relative to HIV2-BEN) and 2TM054B (antisense, 5'-CTTCTGTTTCTTCGTTGGCTGGC-3', 8909–8887) for the first PCR and 2TM053A (sense, 5'-CCG-TCTGGGGAACGAAAAACCTCCAG-3', 8403–8428) and 2TM052B (antisense, 5'-GAGAATACTGGCCTATAGCC-CTT-3', 8835–8813) for the second PCR.

HIV-2 strain (01JP-IMCJ/KR020.1) was isolated from this patient by a standard cocultivation method. Briefly, the PBMCs were separated on Ficoll-Hypaque (Pharmacia, Piscataway, NJ) density gradient centrifugation. PBMCs were cocultured with phytohemagglutinin (PHA, 1 μ g/ml)-stimulated PBMCs from HIV-1 negative healthy donors in RPMI 1640 containing 10% fetal calf serum and interleukin-2 (20 U/ml). HIV production was monitored by reverse transcriptase (RT) assay. 01JP-IMCJ/KR020.1 was a CCR5-utilizing HIV-2 strain with a non-syncytium-inducing phenotype (data not shown).

For further characterization, we cloned and determined the near full-length nucleotide sequence of the HIV-2 proviral genome. Briefly, DNAs were extracted from CD8-depleted PHA-stimulated PBMCs infected with 01JP-IMCJ/KR020.1 by

DNAzol (Invitrogen, Carlsbad, CA). The near full-length HIV-2 genome was amplified by using the Expand Long Template PCR system (Roche Molecular Biochemicals) with the primer set of pbs-496A (sense: 5'-AGTGGGGCCCGAACAGG-3'; *Nar*I site, underlined) and H2U5B (antisense: 5'-AAGGGTC-CTAACAGACCAGGGT-3'). Purified PCR fragments were cloned into pBRTA2, a pBR322-based vector carrying the *Xcm*I site for TA cloning.¹⁴ A positive clone with a near full-length HIV-1 insert was selected and the nucleotide sequence of the HIV-2 genome was determined on both strands by a direct sequencing method with fluorescent dye terminators in an automated ABI PRISM310 DNA sequencer (Applied Biosystems, Inc., Foster City, CA), using the primer-walking approach. The near full-length molecular clone, 01JP-IMCJ/KR020.1.1, had intact open reading frames for all HIV-2 genes, except for the *gag* gene, which contains a frame shift mutation.

The phylogenetic analyses based on *gag* (p17–p24) (Fig. 2A), *env* (gp41) (Fig. 2B), and near full-length (Fig. 2C) nucleotide sequences revealed that 01JP-IMCJ/KR020.1.1 belong to the HIV-2 subtype B cluster with high bootstrap support (81–100%) (Fig. 2A–C). 01JP-IMCJ/KR020.1.1 harbors a 13-nucleotide insertion upstream of the NF- κ B site that is one of the sequence signatures specific to HIV-2 subtype B (Fig. 2D).

This patient does not have any history of travel outside Korea, except for Japan, and had no documented links to the endemic areas of HIV-2 subtype B in the central and eastern part of West Africa (Fig. 3). He most likely acquired HIV-2 sexually through female commercial sex workers (FCSWs) in either

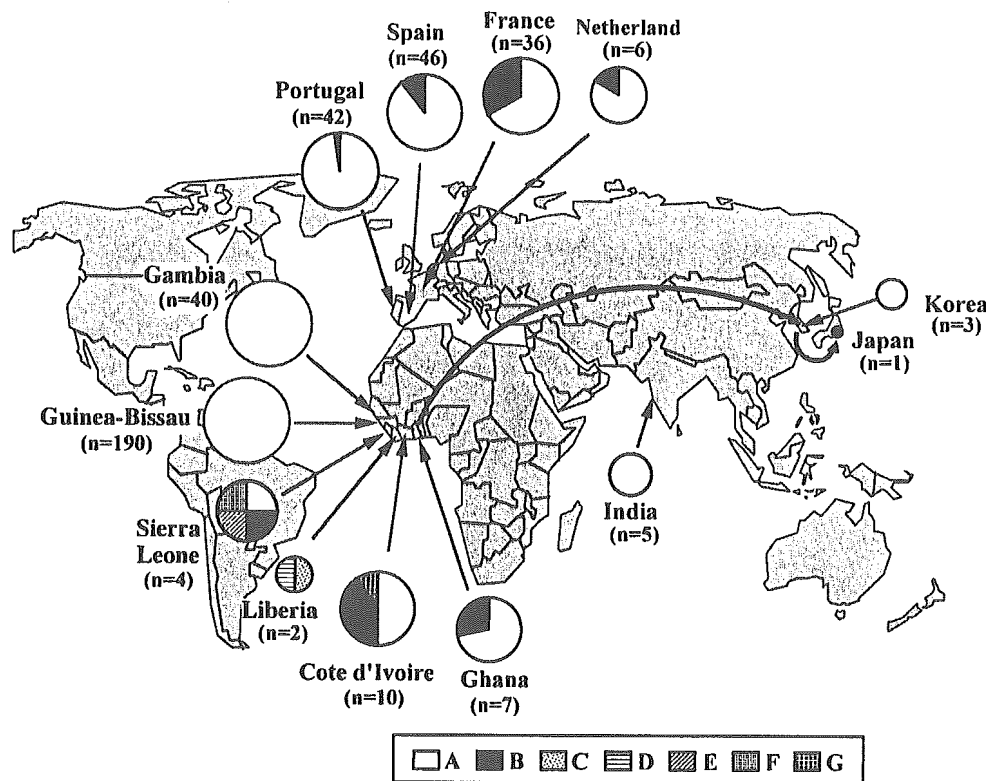


FIG. 3. The distribution of HIV-2 subtypes in Asia and the world. The pies that showed the subtype distribution (see inset) were drawn based on the compiled dataset in the review.¹ One subtype G specimen was found in Ivory Coast.¹⁵

Korea or Japan. Among five HIV-2 cases identified in Korea between 1991 and 1998, three were sailors who were infected through heterosexual contacts with local fCSWs in HIV-2 endemic areas (one case in Senegal; two cases in the Canary Islands). However, the remaining two cases (one male and one female) were thought to have contracted HIV-2 via sexual contacts inside Korea.¹³ Together with our report, we conclude that at least sporadic transmissions of HIV-2 including both subtypes A and B have occurred in East Asia. It is necessary to keep monitoring HIV-2 to see if there is any increasing trend of HIV-2 infection in this region.

The near-full-length nucleotide sequence of 01JP-IMCJ/KR020.1.1 is available under GenBank accession number AB100245.

ACKNOWLEDGMENTS

We thank Koya Ariyoshi for critical reading of the manuscript and Naoki Yamamoto, Naoko Kimura, and Satoshi Kimura for their support. We also thank Yuuko Nishimura and Mikio Mizukoshi of Fujirebio Co. for excellent help with the serological tests. This study was supported by grants from the Ministry of Health, Labour and Welfare and from the Ministry of Education and Science.

REFERENCES

- Schim van der Loeff MF and Aaby P: Towards a better understanding of the epidemiology of HIV-2. *AIDS* 1999;13:S69-84.
- Whittle H, Morris J, Todd J, Corrah T, Sabally S, Bangali J, Ngom PT, Rolfe M, and Wilkins A: HIV-2-infected patients survive longer than HIV-1-infected patients. *AIDS* 1994;8:1617-1620.
- Marlink R, Kanki P, Thior I, Travers K, Eisen G, Siby T, Traore I, Hsieh CC, Dia MC, Gueye EH, *et al.*: Reduced rate of disease development after HIV-2 infection as compared to HIV-1. *Science* 1994;265:1587-1590.
- Ariyoshi K, Jaffar S, Alabi AS, Berry N, van der Loeff MS, Sabally S, N'Gom PT, Corrah T, Tedder R, and Whittle H: Plasma RNA viral load predicts the rate of CD4 T cell decline and death in HIV-2-infected patients in West Africa. *AIDS* 2000;14:339-344.
- Simon F, Matheron S, Tamalet C, Loussert-Ajaka I, Bartczak S, Pepin JM, Dhiver C, Gamba E, Elbim C, Gastaut JA, *et al.*: Cellular and plasma viral load in patients infected with HIV-2. *AIDS* 1993;7:1411-1417.
- Berry N, Ariyoshi K, Jaffar S, Sabally S, Corrah T, Tedder R, and Whittle H: Low peripheral blood viral HIV-2 RNA in individuals with high CD4 percentage differentiates HIV-2 from HIV-1 infection. *J Hum Virol* 1998;1:457-468.
- O'Donovan D, Ariyoshi K, Milligan P, Ota M, Yamuah L, Sarge-Njie R, and Whittle H: Maternal plasma viral RNA levels determine marked differences in mother-to-child transmission rates of HIV-1 and HIV-2 in The Gambia. MRC/Gambia Government/University College London Medical School working group on mother-child transmission of HIV. *AIDS* 2000;14:441-448.
- Gao F, Yue L, Robertson DL, Hill SC, Hui H, Biggar RJ, Nequaye AE, Whelan TM, Ho DD, and Shaw GM: Genetic diversity of human immunodeficiency virus type 2: Evidence for distinct sequence subtypes with differences in virus biology. *J Virol* 1994;68:7433-7447.
- Chen Z, Luckay A, Sodora DL, Telfer P, Reed P, Gettie A, Kanu JM, Sadek RF, Yee J, Ho DD, Zhang L, and Marx PA: Human immunodeficiency virus type 2 (HIV-2) seroprevalence and characterization of a distinct HIV-2 genetic subtype from the natural range of simian immunodeficiency virus-infected sooty mangabeys. *J Virol* 1997;71:3953-3960.
- Berry N, Ariyoshi K, Balfe P, Tedder R, and Whittle H: Sequence specificity of the human immunodeficiency virus type 2 (hiv-2) long terminal repeat u3 region in vivo allows subtyping of the principal HIV-2 viral subtypes a and b. *AIDS Res Hum Retroviruses* 2001;17:263-267.
- Pfutzner A, Dietrich U, von Eichel U, von Briesen H, Brede HD, Maniar JK, and Rubsamen-Waigmann H: HIV-1 and HIV-2 infections in a high-risk population in Bombay, India: Evidence for the spread of HIV-2 and presence of a divergent HIV-1 subtype. *J Acquir Immune Defic Syndr* 1992;5:972-977.
- Grez M, Dietrich U, Balfe P, von Briesen H, Maniar JK, Mahambre G, Delwart EL, Mullins JI, and Rubsamen-Waigmann H: Genetic analysis of human immunodeficiency virus type 1 and 2 (HIV-1 and HIV-2) mixed infections in India reveals a recent spread of HIV-1 and HIV-2 from a single ancestor for each of these viruses. *J Virol* 1994;68:2161-2168.
- Kim SS, Kim EY, Park KY, Suh SD, Park HK, Shin YO, Bae M, and Lee JS: Introduction of human immunodeficiency virus 2 infection into South Korea. *Acta Virol* 2000;44:15-22.
- Marchuk D, Drumm M, Saulino A, and Collins FS: Construction of T-vectors, a rapid and general system for direct cloning of unmodified PCR products. *Nucleic Acids Res* 1991;19:1154.
- Yamaguchi J, Devare SG, and Brennan CA: Identification of a new HIV-2 subtype based on phylogenetic analysis of full-length genomic sequence. *AIDS Res Hum Retroviruses* 2000;16:925-930.

Address reprint requests to:

Yutaka Takebe
 Laboratory of Molecular Virology and Epidemiology
 AIDS Research Center
 National Institute of Infectious Diseases
 Toyama 1-23-1
 Shinjuku, Tokyo 162-8640, Japan

E-mail: takebe@nih.go.jp



RESEARCH ARTICLE

DNA vaccine-encapsulated virus-like particles derived from an orally transmissible virus stimulate mucosal and systemic immune responses by oral administration

S Takamura¹, M Niikura², T-C Li³, N Takeda³, S Kusagawa⁴, Y Takebe⁴, T Miyamura³ and Y Yasutomi¹

¹Department of Bioregulation, Mie University School of Medicine, Mie, Japan; ²Department of Virology I, National Institute of Infectious Diseases, Tokyo, Japan; ³Department of Virology II, National Institute of Infectious Diseases, Tokyo, Japan; and ⁴Laboratory of Molecular Virology and Epidemiology, AIDS Research Center, National Institute of Infectious Disease, Tokyo, Japan

Delivery of foreign genes to the digestive tract mucosa by oral administration of nonreplicating gene transfer vectors would be a very useful method for vaccination and gene therapy. However, there have been few reports on suitable vectors. In the present study, we found that plasmid DNA can be packaged *in vitro* into a virus-like particle (VLP) composed of open reading frame 2 of hepatitis E virus, which is an orally transmissible virus, and that these VLPs can deliver this foreign DNA to the intestinal mucosa *in vivo*. The delivery of plasmid DNA to the mucosa of the small intestine was confirmed by the results of immunohistochemical analyses using an expression plasmid encoding human immunodeficiency virus *env* (HIV *env*) gp120. After oral administration of VLPs loaded with HIV *env* cDNA, significant levels of specific IgG and IgA to HIV *env* in fecal extracts and sera were found. Moreover, mice used in this study exhibited cytotoxic T-lymphocyte responses specific to HIV *env* in the spleen, Payer's patches and mesenteric lymph nodes. These findings suggest that VLPs derived from orally transmissible viruses can be used as vectors for delivery of genes to mucosal tissue by oral administration for the purpose of DNA vaccination and gene therapy.

Gene Therapy (2004) 11, 628–635. doi:10.1038/sj.gt.3302193
Published online 19 February 2004

Keywords: VLP; oral DNA vaccine; CTL; HIV; mucosal immunity

Introduction

The successful outcome of novel gene therapies and DNA vaccinations largely depends on the development of effective delivery systems.¹ In human applications, both the efficacy and safety of any delivery system used for gene transfer are major concerns. It has been shown that tissue-specific gene transfer by a viral vector could be achieved naturally and effectively through cell specificity of the virus receptors.² However, there is a risk of vector toxicity through viral infection of the host cells. Also, the limited sizes of transgenes often present a serious obstacle. Nonviral vectors, such as liposomes, are safer but do not have a cell-specific targeting component and have limited transduction both *in vitro* and *in vivo*. This limitation has been partly overcome by the development of molecular conjugates consisting of cell-specific ligands that confer cell specificity to nonviral vectors.^{3,4}

The development of a system for delivering genes to or conferring immunity to mucosal tissue by oral administration would provide a convenient means for effective treatment or prevention of various human

diseases, including cancers, infectious diseases and immunological disorders.⁵ Since many pathogenic viruses and bacteria establish their initial infections through the mucosal surface, vaccine strategies that can stimulate mucosal immunity have been widely studied (reviewed in Ogra *et al*).⁶ However, there are several difficulties in oral immunization with nonreplicating molecules, such as low pH in the stomach, the presence of proteolytic enzymes in the digestive tract and the presence of physical as well as biochemical barriers associated with the mucosal surface itself.⁶

Among the various nonreplicating molecules, a virus-like particle (VLP), an empty particle with a structure similar to that of an authentic virus particle, offers the possibility of a new approach for vaccine development.⁷ It is expected that the VLP structure will provide resistance to severe environments in the digestive tracts and enable specific binding to the mucosal surface if an appropriate VLP is chosen.⁸ However, VLPs can induce immune responses to themselves, and this is a problem for using VLPs as a vaccine vector to carry foreign DNA. A system using polyoma virus VP1 VLPs as a carrier of DNA by intranasal administration has been reported.⁹ These VLPs work as an adjuvant, since DNA vaccine can induce immune responses by intranasal administration without VLPs. Hepatitis E virus (HEV) is an unclassified calicivirus-like, positive-strand RNA virus that causes

Correspondence: Y Yasutomi, Department of Bioregulation, Mie University School of Medicine, 2-174 Edobashi, Tsu, Mie 514-8507, Japan
Received 27 March 2003; accepted 21 October 2003

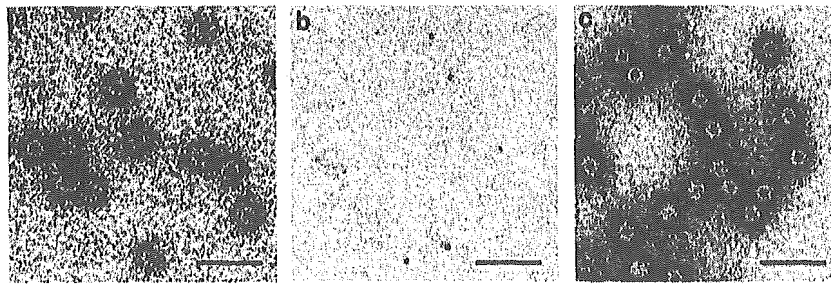


Figure 1 Electron micrographs of HEV-VLPs: (a) purified HEV-VLPs before treatment; (b) disassembled HEV-VLPs after treatment of VLPs with EGTA and DTT; and (c) refolded HEV-VLPs in the presence of CaCl_2 , DMSO and DNA. Bars represent 50 nm.

human acute hepatitis by fecal–oral transmission. HEV first infects epithelial cells of the small intestine and then reaches the liver through the portal vein. It has recently been reported that overexpression of a part of open reading frame 2 (ORF2) in a baculovirus expression system results in the assembly of this protein into a VLP.¹⁰ We have also reported that VLPs carrying foreign epitopes elicit strong mucosal and systemic immune responses to both the VLPs and exogenous epitopes without the requirement of any kind of adjuvant when orally administered to mice.¹¹

Since infection with human immunodeficiency virus (HIV) most likely occurs through exposure of mucosal tissue to the virus, HIV-specific immune responses at mucosal sites are critical for the initial control of infection. Therefore, a nonreplicating vaccine vector that elicits mucosal immunity by oral administration would be a powerful HIV vaccine. In the present study, we found that unrelated plasmid constructs can be encapsulated into HEV-VLPs and delivered to the intestinal mucosa by oral administration. HIV DNA vaccine-loaded HEV-VLPs can elicit mucosal and systemic cellular as well as humoral immune responses by oral administration.

Results

In vitro refolding of VLPs

The HEV-VLPs produced by a recombinant baculovirus system were disassembled by the removal of calcium ions (Figure 1b). When calcium ions were supplemented to the disrupted VLPs in the presence of plasmid DNA, the DNA was encapsulated into the refolded VLPs (Figure 1c). No significant morphological difference due to the VLP disassembling–refolding process was observed under an electron microscope.

Density shifts of VLPs and amount of plasmid DNA after DNA encapsulation

Plasmid DNA encapsulation in the refolded VLPs was confirmed by CsCl equilibrium gradient centrifugation. VLP density is greater when loaded with a DNA plasmid. A heavier density gradient peak was present only when DNA was incorporated into the VLPs (Figure 2d). A single lighter density peak was produced for VLPs alone (Figure 2a), refolded VLPs (Figure 2b) and intact VLPs in the presence of plasmid DNA (Figure 2c). Despite the various sizes of plasmid DNA used for

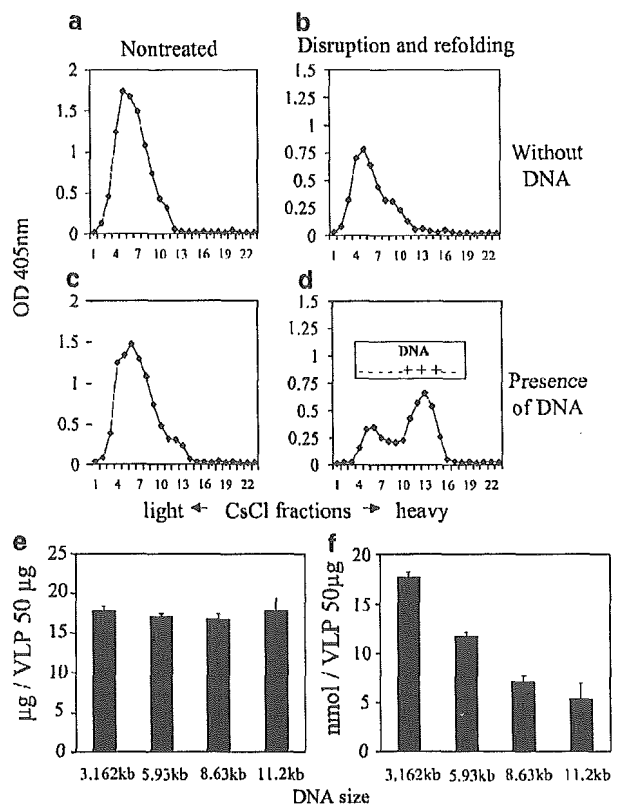


Figure 2 CsCl gradient profiles of intact and refolded VLPs. No DNA added: (a) intact; (b) refolded. DNA added: (c) intact; (d) refolded. The amount of DNA encapsulated in VLPs is expressed as μg (e) and molality (f) per 50 μg VLP protein.

encapsulation, the amounts of plasmid in VLPs were almost the same (17–19 μg per 50 μg of HEV-VLPs) (Figure 2e and f). A solution with a high concentration of plasmid DNA showed high viscosity, and VLPs including DNA were not obtained for general use in experiments. Based on these results, we used this amount (1 mg/ml) as the optimal concentration (data not shown).

Gene transfer by HEV-VLPs

Initially, four cell lines derived from mice, rabbits, monkeys and humans were studied for their ability to

transfer genes *in vitro*. The fluorescence of GFP-expressing cells was observed under a fluorescence microscope. Although the percentages of fluorescence-positive cells were not so high (11.2% of NIH3T3 cells, 19.6% of RK-13 cells, 21.0% of COS-7 cells and 20.1% of HepG2 cells), all of the cell lines used in this study showed positive reactions (Figure 3). In contrast, no fluorescence-positive cells were observed when the cells were incubated with plasmid DNA alone or intact VLPs in the presence of plasmid DNA (data not shown). We next tried gene transduction *in vivo*. Mice that had orally received a vaccine of DNA expressing HIV env gp120 of the NL432 strain (pJWNL432) that was encapsulated in VLPs were killed 2 days after immunization, and the expression of HIV env protein in the digestive tract was examined. HIV env protein was found in epithelial cells of the small intestine by immunohistochemistry (Figure 4), indicating that the HEV structure necessary for the entry of HEV into target cells had been preserved in refolded VLPs and that the DNA encapsulated in HEV-VLPs had been delivered to intestinal tissues.

Systemic and mucosal HIV-specific humoral immune responses in mice that had orally received a vaccine of HIV DNA encapsulated in VLPs

Mice were orally or subcutaneously immunized four times at 1-week intervals with pJWNL432 either naked or encapsulated in HEV-VLPs. The serum levels of HIV env-specific IgG antibodies in mice that had received loaded VLPs were significantly higher than those in mice that had received naked DNA ($P < 0.05$ at 12 wpi, Figure 5a and e). Moreover, specific IgA was detected at high levels in sera of mice that had received loaded VLPs but not in sera of mice that had been immunized subcutaneously ($P < 0.05$ at 12 wpi, Figure 5b and f). HIV env-specific IgA was only detected in fecal extracts of mice that had orally received pJWNL432-encapsulated HEV-VLPs (Figure 5d and h). No specific IgG was detected in any of the fecal

samples (Figure 5c and g). The levels of HIV env-specific IgG antibodies detected in sera from subcutaneously and orally immunized mice were the same (Figure 5a and e). HEV-specific IgA was detected in both sera and fecal extracts of mice that had been orally administered VLP but not in sera or fecal extracts of mice that had been immunized subcutaneously (Figure 5j and l). Both orally and subcutaneously immunized mice showed HEV-specific IgG in sera (Figure 5i) and fecal extracts (Figure 5k).

Elicitation of HIV-specific cytotoxic T lymphocytes at systemic and mucosal sites by oral administration of a vaccination of HIV DNA encapsulated in VLPs

Cytotoxic T lymphocyte (CTL) responses in the spleen, mesenteric lymph nodes (MLN) and Payer's patches (PP) were investigated at 5 weeks after the first immunization. Mice that had orally received pJWNL432 encapsulated in HEV-VLPs showed HIV env epitope-specific CTL responses in the spleen, MLN and PP, whereas cells from the same tissues in mice that had received naked DNA vaccine did not show any CTL activity (Figure 6a). The P18 peptide is a dominant HIV env CTL and Th cell epitope in BALB/c mice and is restricted to the H-2D^d allele. These effector cell functions derived from our experiments were inhibited by either anti-CD8 or -H-2D^d monoclonal antibody (mAb) (Figure 6b,c), indicating that oral immunization of mice with a vaccine of HIV env DNA-encapsulated HEV-VLPs elicited CD8⁺ and MHC class I-restricted CTLs both locally and systemically.

Discussion

A large number of pathogens gain access to the human body via mucosa such as oral, nasal or genital mucosa. The best defense against these predominantly mucosal

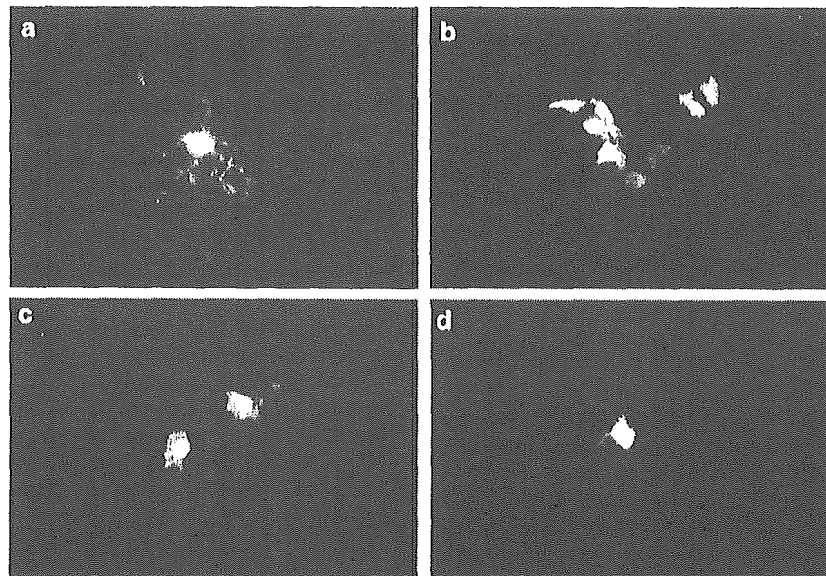


Figure 3 Expression of GFP in cells transfected with plasmid DNA encapsulated in HEV-VLPs: (a) NIH/3T3 cells (mouse); (b) RK-13 cells (rabbit); (c) COS-7 cells (monkey); and (d) HepG2 cells (human).

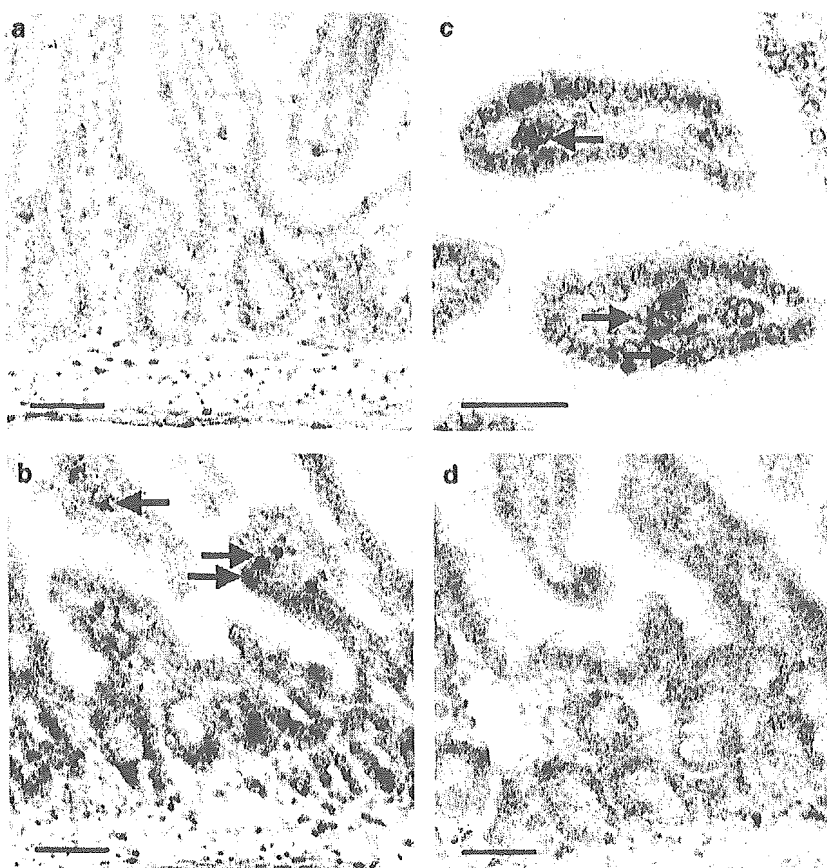


Figure 4 Immunostaining of serial sections of small intestine tissue from mice 2 days after oral administration of pJWNL432-encapsulated VLPs. HIV *env* proteins were observed in epithelial cells (arrow) (b, c), and control mAb did not show any positive reactions (d). Control mice were also administered pJWNL432 without VLP encapsulation (a). Bar marker represents 50 μ m.

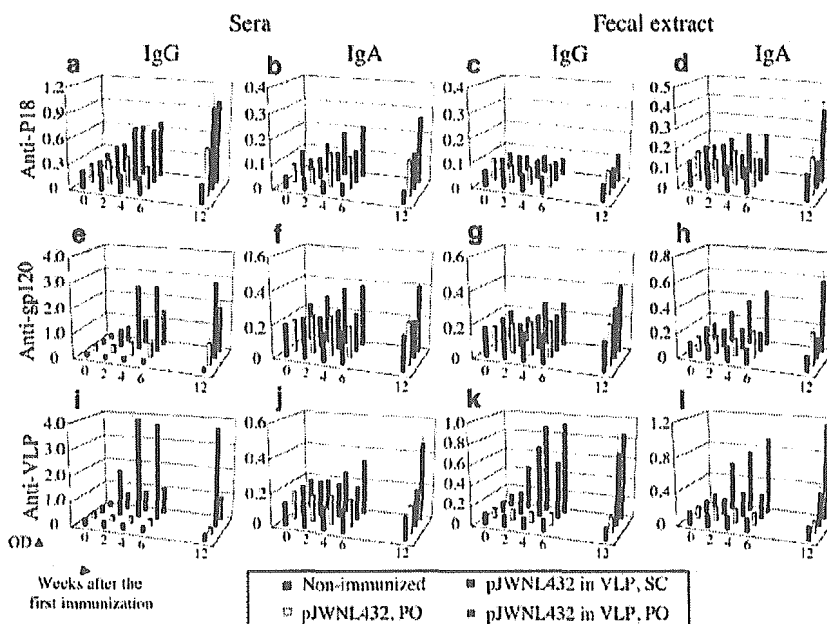


Figure 5 IgG (a, c, e, g, i and k) and IgA (b, d, f, h, j and l) levels in sera (a, b, e, f, i and j) and fecal extracts (c, d, g, h, k and l) of immunized mice. Mice were orally (▨) or subcutaneously (■) administered pJWNL432 encapsulated in VLP or naked (□). Symbols indicate HIV *env*-specific antibody levels. Background levels to HIV *env* in nonimmunized mice (▤) are also shown. The IgG and IgA antibody levels are expressed as OD at dilutions of 1:100 and 1:2 for serum and fecal extracts, respectively. The mean OD values \pm s.e.s were obtained from five mice/group.

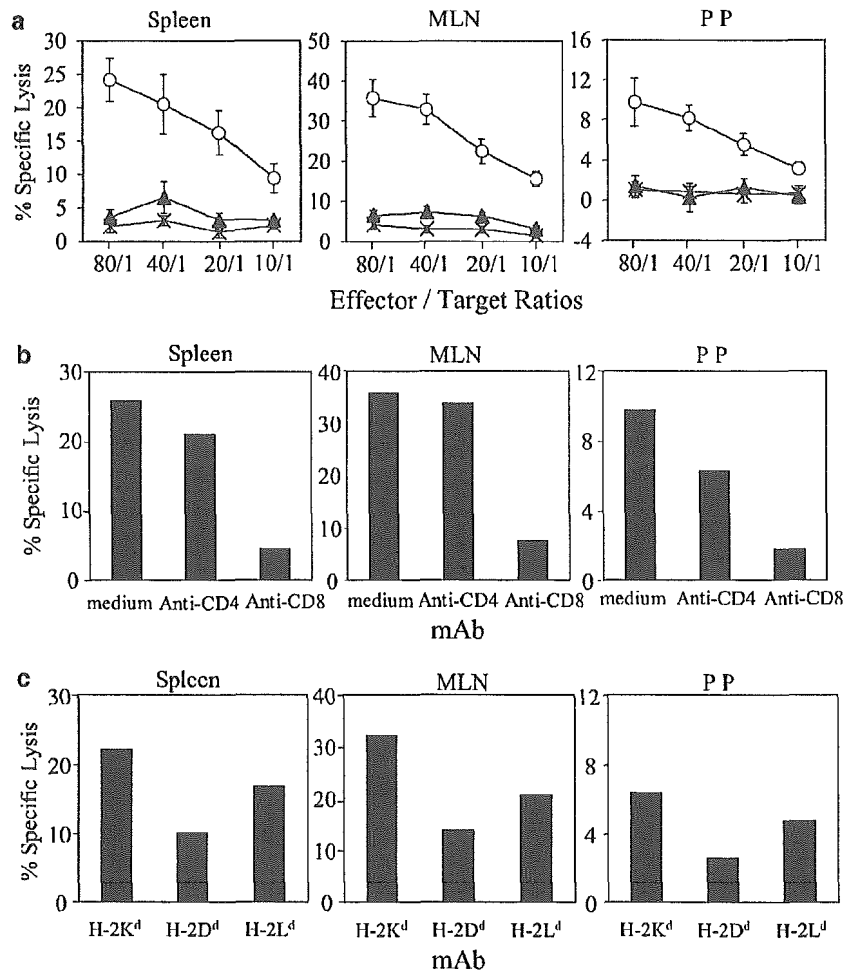


Figure 6 Spleen, MLN and PP cells from mice orally administered pJWNL432-encapsulated VLPs elicited CTL. (a) Mice were orally administered pJWNL432 encapsulated in VLPs (circles) or naked (triangles). Results for nonimmunized controls are also shown (x). (b) Effector cells obtained from the spleen, MLN and PP cells of mice orally administered pJWNL432-encapsulated VLPs are mediated CD8⁺ cells. Lytic activities of effector cells were assessed in the presence of anti CD4 mAb, anti-CD8 mAb or medium. Effector:target ratio was 80:1. (c) HIV *env*-specific lysis was restricted by MHC class I. Effector cells were examined for P18-specific lytic activities in the presence of anti-H-2K^d, anti-H-2D^d or H-2L^d mAb. The percentage of P18-specific lysis was calculated as (% lysis of target cells labeled with P18)–(% lysis of target cells labeled with control peptide). Each value is the mean percentage of the specific lysis values obtained from five mice.

pathogens is mucosal vaccines that are capable of inducing both systemic and mucosal immunity. Recent evidence has shown that DNA vaccination can confer protection against a number of infectious agents, including viruses and bacteria, although peripheral immunization with naked DNA is less than optimal for stimulating mucosal immunity.^{12,13} In fact, it is quite difficult to induce both mucosal and systemic immune responses by oral administration of naked DNA. This study demonstrated that an orally administered DNA vaccine encapsulated in an orally transmissible virus-derived VLP induced both mucosal and systemic immunity.

The delivery of a DNA vaccine for induction of mucosal immune responses is usually achieved by gene transfer to the upper nasopharynx-associated lymphoid tissue (NALT), upper airway, salivary glands and tonsils.^{5,14} Despite its obvious convenience, oral administration is rarely successful, since it is quite difficult to protect plasmid DNA from the environment in the

digestive tract. The efficacy of orally delivered DNA vaccine to NALT is improved by encapsulating plasmid DNA in poly (lactide-coglycolide) (PLG) microparticles for protection against the gastric environment.^{15,16} The immune responses to particle-borne DNA immunizations by means such as utilization of a gene gun or PLG differ from those to DNA immunizations without particles.¹³ It is thought that the microparticles are actively taken up by cells such as macrophages or M cells of the small intestine and thus facilitate the presentation of antigens to local immune systems.^{15,17} This mechanism is the same as that of gene gun immunization of a DNA vaccine, that is, phagocytic cells such as macrophages or dendritic cells take up plasmid DNA delivered by a gene gun. The delivered gene is expressed only in these cells.¹⁸ Similarly, only mucosal immunity was induced in mice by oral administration of DNA-encapsulated PLG microparticles.^{15,16} It is likely that the mechanism underlying immune recognition of

HEV-VLP infection is similar to that of direct intramuscular or subcutaneous DNA immunization without the use of particles. Protein expressed by HEV-VLP-infected cells is recognized by the immune surveillance system, resulting in the elicitation of Ag-specific immune responses. We showed in this study that genes could be expressed in epithelial cells in the small intestine after delivery by HEV-VLPs (Figure 4). It is plausible that HEV-VLPs, which are derived from an orally transmissible virus, were incorporated into HEV-permissive epithelial cells in the small intestine, because they retained structures and properties similar to those of HEV particles, producing an infection similar to that induced naturally.¹⁹ The Ag-expressing cells might be recognized by intraepithelial lymphocytes or submucosal antigen-presenting cells by the same mechanism as that in the case of general virus infection.

An HEV-VLP has several advantages as a vector of DNA. Firstly, in our experience, large amounts can be easily obtained from standard cultivation protocols compared with the amounts of other VLPs obtained. The yield of purified HEV-VLPs collected from a culture supernatant of 50–100 µg/ml is more than 100 times greater than that of other VLPs. Secondly, the outcome of gene delivery in humans can be predicted using conventional laboratory animals, since HEV naturally infects various animals as well as humans through the same infectious route and target cells.^{10,20} Thirdly, HEV-VLPs are stable at room temperature. Fourthly, anti-HEV immune responses had no effect on DNA administration in the present study, and this might be related to the neutralizing antibody for preventing infection with HEV. Neutralizing antibodies to HEV for inhibiting infection have not yet been found. This is also the case for HCV. The mechanism by which HEV is eliminated by antibodies is thought to be antibody-dependent cell-mediated cytotoxicity (ADCC). The effect of induction of immune responses to DNA vaccine in our system is not clear. Thus, HEV-VLPs are an attractive vaccine vector in developing countries because these VLP can be preserved without the requirement of any particular equipment. Finally, we have reported that an HEV-VLP can carry foreign amino-acid sequences as a part of the ORF2 protein exposed on the particle surface without any morphological or biological alteration.¹⁰ Liposomal vectors resembling retroviral envelopes endowed with targeting molecules for gene delivery have been reported. The vicronectin receptor, $\alpha_v\beta_3$ -integrin, is commonly upregulated on malignant melanoma cells, and liposome carrying an Arg-Gly-Asp (RGD) integrin-binding motif has been used for a system to deliver DNA to these tumor cells.²¹ It has also been reported that targeting DNA to M cells by intranasal administration for the induction of mucosal and systemic responses can be achieved by formulating DNA with polylysine linked to viral adhesion.²² It may be possible to design chimeric ORF2 proteins carrying these targeting molecules to re-target HEV-VLP to particular cell types.

Oral vaccination has obvious advantages for a field trial in a large-scale public health vaccination program.²³ From a practical standpoint, oral administration is less stressful for vaccine recipients and does not require professional skill for the vaccine administration. Moreover, delivery of vaccines via the intestinal tract is considered to be inherently safer than systemic injection.

Encouraging results of phase I trials using Norwalk virus VLPs have recently been reported.²⁴ Trials using DNA vaccines for infectious and malignancy diseases have also been conducted.²⁵ The results of the present study suggest that oral administration of DNA vaccine encapsulated in oral transmissible virus VLPs, HEV-VLPs, is effective for inducing both humoral and cellular immunity locally as well as systemically. HEV-VLPs might be useful not only for vaccination but also as a vector in human gene therapy.

Materials and methods

Mice

BALB/c female mice were purchased from Clea Japan (Tokyo, Japan) and were housed in the Laboratory Animal Center of Mie University School of Medicine during the experimental period.

Peptide synthesis

The peptides used in this study were the HIV env CTL epitope (HIV 308-322, RIQRGPGRAFTIGK; P18)²⁶ and a control peptide (HCV nonstructural protein 5 CTL epitope MSYSWTGALVTPCAAEE; P17).²⁷

Plasmid DNA

A highly efficient mammalian expression vector, pJW4303,²⁸ was used for efficient expression of HIV env gp120 of the NL432 strain.²⁹ Various sizes of plasmid DNA were also used for the *in vitro* packaging experiment (3.162 kb: pUC118; 5.93 kb: pJW322; 8.63 kb: pJWSIVenv; 11.2 kb: pABWN).

Production and purification of HEV-VLPs

HEV-VLPs were produced and purified by previously described methods.^{10,11} Briefly, Tn5 cells maintained in Excel 405 serum-free medium (JRH, KS) were infected with the recombinant baculovirus expressing HEV-ORF2 at an m.o.i. of >5 and cultured for 6 days. The supernatant was harvested and the recombinant baculovirus in the supernatant was pelleted by ultracentrifugation at 10 000 g for 30 min at 4°C. The VLPs in the supernatant were collected by further ultracentrifugation at 100 000 g for 2 h at 4°C. Pelleted VLPs were then resuspended in 10 mM potassium-[2-(*N*-morpholino)ethanesulfonic acid] (MES) buffer (pH 6.2) and purified on a CsCl equilibrium density gradient. The purified HEV-VLPs were spun down and resuspended in potassium-MES buffer and kept at 4°C.

DNA packaging

Plasmid DNA was encapsulated into HEV-VLPs according to a previously described procedure.³⁰ Purified VLPs (50 µg) were disrupted by incubation in 180 µl of a buffer containing 50 mM Tris-HCl (pH 7.5), 150 mM NaCl, 1 mM EGTA and 20 mM dithiothreitol. Following 30 min of incubation at room temperature, 200 µg (20 µl) of each plasmid in 50 mM Tris-HCl buffer (pH 7.5) and 150 mM NaCl was added. The disrupted VLP preparation was refolded by incubation for 1 h with increasing concentrations of CaCl₂ up to a final concentration of 5 mM. VLPs were pelleted by ultracentrifugation and resuspended in 10 mM potassium-MES buffer (pH 6.2). At each step, the VLP structure formation was confirmed by electron